Condensation of electron-hole pairs in a two-layer graphene system: Correlation effects

Yu. E. Lozovik,[1,2,*] S. L. Ogarkov,[3] and A. A. Sokolik[1]

[1]*Institute for Spectroscopy, Russian Academy of Sciences, 142190 Troitsk, Moscow region, Russia*

[2]*Moscow Institute of Physics and Technology, 141700 Dolgoprudny, Moscow region, Russia*

[3]*National Nuclear Research University "MEPHI," 115409 Moscow, Russia*

(Received 19 February 2012; revised manuscript received 21 May 2012; published 20 July 2012)

Condensation of pairs formed by spatially separated electrons and holes in a system of two isolated graphene layers is studied beyond the mean-field approximation. Suppression of the screening of the pairing interaction at large distances, caused by the appearance of the gap, is considered self-consistently. A mutual positive feedback between the appearance of the gap and the enlargement of the interaction leads to a sharp transition to a correlated state with a greatly increased gap above some critical value of the coupling strength. At a coupling strength below the critical value, this correlation effect increases the gap approximately by a factor of 2. The maximal coupling strength achievable in experiments is close to the critical value. This indicates the importance of correlation effects in closely spaced graphene bilayers at weak substrate dielectric screening. Another effect beyond the mean-field approximation considered is the influence of vertex corrections on the pairing, which is shown to be very weak.

DOI: 10.1103/PhysRevB.86.045429 PACS number(s): 73.22.Pr, 71.35.−y, 74.20.−z, 73.21.−b

I. INTRODUCTION

Pairing of spatially separated electrons and holes caused by their Coulomb attraction was proposed initially as a possible origin of superfluidity,[1] Josephson effects,[1–3] and anomalous electromagnetic phenomena[4,5] in coupled semiconductor quantum wells. In the case of a dense electron-hole system, this pairing is similar to Cooper pairing of electrons in superconductors and to electron-hole pairing in excitonic insulators.[6] Strong Coulomb electron-hole attraction was supposed to maintain a high critical temperature of the pairing, while spatial separation of paired electrons and holes could prevent them from interlayer tunneling, leading to their recombination and to a condensate phase fixation. Experimental evidences of a superfluid transition in two-layer semiconductor structures in a strong magnetic field (pairing of composite fermions)[7] and without magnetic field[8–12] were found several decades later.

Fabrication of graphene, an atomically thin two-dimensional form of carbon,[13,14] makes it possible to realize electron-hole pair condensation in a system of two graphene layers isolated from each other (hereafter referred to as a "graphene bilayer"). Structures consisting of two independently gated graphene layers with common contacts and very small (0.6 nm) separation have been fabricated and studied experimentally.[15,16] A system of two independently contacted graphene layers separated by a 5-nm-thick SiO_2 barrier has also been made,[17] and Coulomb drag has been studied in such a system. The most promising systems to realize the pairing could be heterostructures consisting of two graphene layers separated by an atomic thin boron nitride layer. Considerable progress in the fabrication of such structures with ultrahigh mobility encapsulated graphene samples has been achieved recently.[18–22] Measurements of Coulomb drag in these structures have been reported (see Ref. 23 and references therein).

Theoretical studies of electron-hole pair condensation in a spatially separated graphene bilayer were presented in Refs. 24–33. It was shown that both weak and strong coupling regimes of the pairing are achievable experimentally.[24] Estimates of the critical temperature T_c at strong coupling[25–30] are very dependent on the model and approximations used, ranging from room temperature, with the unscreened Coulomb attraction taken as a pairing potential,[25,26] to unobservably small values given by Bardeen-Cooper-Shrieffer (BCS) theory with screened interaction.[27]

The pairing in a graphene bilayer at strong coupling was argued[28,29,33] to involve both conduction and valence bands of electrons and holes, i.e., it is multiband. This is due to the fact that electrons and holes in graphene are described by an effective two-dimensional Dirac-type equation for massless particles,[13,14] and thus a gap between the conduction band and the valence band is absent. It was shown[28,29,33] that in this case, T_c can be much larger than that given by the one-band BCS-like model.[27] A study of the problem, taking into account the effects of the frequency dependence of the gap and the pairing potential, was presented in Ref. 30.

The mean-field approximation used in most theoretical works[24–30,33] is known to be well-applicable at both the weak and strong coupling sides of the BCS-BEC (Bose-Einstein condensate) crossover, taking place in conventional pairing systems.[34] However, little is known about its applicability in the regime of multiband Cooper pairing, which takes place in a graphene bilayer at strong coupling instead of the BEC side of the crossover[29,35] (the BEC regime is restored in a graphene bilayer if a gap is opened in its spectrum).[36,37]

One of the correlation effects arising beyond the mean-field approximation is suppression of the screening (and the consequent enhancement of the electron-hole interaction) due to the appearance of the gap and the order parameter in the system. As supposed in Ref. 31, mutual positive feedback between the onset of the gap and suppression of the screening can result in the appearance of two solutions of the gap equation: a small gap at strong screening and a large gap at weak screening.

Changes in the electron system polarizability caused by the appearance of a gap in its spectrum have been studied extensively in the context of collective modes in

superconductors (see, e.g., Refs. 38 and 39) and phonon self-energies, acquiring sharp features at frequencies twice as large as the gap (see Refs. 40 and 41 and references therein).

In systems with electron-hole pairing (proposed initially as an origin of an excitonic insulator),[6] suppression of polarizability due to the pairing can change the pairing interaction significantly. The self-consistent treatment of pairing and screening in electron-hole liquids in semiconductors has been addressed in several works.[42–46]

Suggested in Ref. 31 for an electron-hole graphene bilayer, the self-consistent suppression of the screening was considered in Ref. 32 within the one-band approximation, however without providing details of the calculations. It was shown that for a considered range of parameters, this effect is negligible and the gap equation has only one solution, corresponding to a very small gap. In the present article, we study this effect within the model of multiband pairing at strong coupling. Our results obtained with this model indicate, in contrast to Ref. 32, that the self-consistent suppression of the screening can drastically change the characteristics of the pairing at strong enough coupling, opening up the possibility of the formation of a very large gap.

The self-consistent suppression of the screening is described by a series of Feynman diagrams, involving the screening of the electron-hole interaction by virtual Bogolyubov excitations. A considerable part of the remaining diagrams beyond the mean-field Gor'kov equations can be absorbed into renormalization of a Coulomb interaction vertex. In the theory of superconductivity, this renormalization is negligible at weak coupling due to the Midgal theorem, but it can be significant at strong coupling, generally increasing critical temperature.[47] Corrections to the Coulomb interaction vertex in graphene were considered in Refs. 48–51. It was shown that corrections are large in undoped graphene[49] but rather small at finite doping.[50] We calculate numerically the simplest vertex correction and show that it increases the coupling strength slightly.

The article is organized as follows. In Sec. II, we introduce briefly the multiband model of the pairing. In Sec. III, we consider self-consistent suppression of the screening and its effect on the pairing at zero temperature. Section IV presents calculations of the vertex corrections, and Sec. V concludes the article.

II. MULTIBAND DESCRIPTION OF THE PAIRING

Multiband pairing of electrons and holes in a graphene bilayer at strong coupling is described in detail elsewhere.[28,29,33] Here we present only the formulas needed for further calculations.

To describe the pairing, we introduce the Matsubara Green functions $G^{(ij)}_{\gamma_1\gamma_2}(\mathbf{p},\tau) = -\langle T c^{(i)}_{\mathbf{p}\gamma_1}(\tau) c^{(j)+}_{\mathbf{p}\gamma_2}(0)\rangle$, where $c^{(1)}_{\mathbf{p}\gamma} \equiv a^{(1)}_{\mathbf{p}\gamma}$, $c^{(2)}_{\mathbf{p}\gamma} \equiv a^{(2)}_{\mathbf{p},-\gamma}$, and $a^{(1)}_{\mathbf{p}\gamma}$ and $a^{(2)}_{\mathbf{p}\gamma}$ are destruction operators of electrons in electron- and hole-doped layers, respectively, with the momentum $\mathbf{p}$ from the conduction ($\gamma = +1$) or valence ($\gamma = -1$) band. The bare Green functions for electrons and holes are $G^{(ii)}_{\gamma_1\gamma_2}(\mathbf{p},i\varepsilon_n) = \delta_{\gamma_1\gamma_2}[i\varepsilon_n - \xi^{(i)}_{\mathbf{p}\gamma_1}]^{-1}$, where $\xi^{(1)}_{\mathbf{p}\gamma} = -\xi^{(2)}_{\mathbf{p}\gamma} \equiv \xi_{p\gamma} = \gamma v_F p - \mu$ are energies of electrons and holes measured from the chemical potentials μ and $-\mu$ in electron- and hole-doped graphene layers, respectively; $v_F \approx 10^6$ m/s is the Fermi velocity in graphene.

In the simplest case of s-wave band-diagonal pairing, all the Green functions $G^{(ij)}_{\gamma_1\gamma_2}$ are nonzero only at $\gamma_1 = \gamma_2$. The solution of the Gor'kov equations in the Cooper channel in this case is

$$G^{(11)}_{\gamma\gamma}(\mathbf{p},i\varepsilon_n) = \frac{u^2_{p\gamma}}{i\varepsilon_n - E_{p\gamma}} + \frac{v^2_{p\gamma}}{i\varepsilon_n + E_{p\gamma}}, \tag{1}$$

and $G^{(22)}_{\gamma\gamma}(\mathbf{p},i\varepsilon_n) = -G^{(11)}_{\gamma\gamma}(\mathbf{p},-i\varepsilon_n)$, $G^{(12)}_{\gamma\gamma}(\mathbf{p},i\varepsilon_n) = G^{(21)}_{\gamma\gamma}(\mathbf{p},i\varepsilon_n)$. Conventional notations for coherence factors and Bogolyubov energies are used:

$$u^2_{p\gamma} = \frac{1}{2}\left(1 + \frac{\xi_{p\gamma}}{E_{p\gamma}}\right), \quad v^2_{p\gamma} = \frac{1}{2}\left(1 - \frac{\xi_{p\gamma}}{E_{p\gamma}}\right),$$
$$u_{p\gamma}v_{p\gamma} = \frac{\Delta_{p\gamma}}{2E_{p\gamma}}, \quad E_{p\gamma} = \sqrt{\xi^2_{p\gamma} + \Delta^2_{p\gamma}}. \tag{2}$$

Note that in the multiband regime, we have two branches of the gap functions $\Delta_{p\pm}$ and Bogolyubov excitation energies $E_{p\pm}$ corresponding to conduction and valence bands.

The gap functions are determined by the equation

$$\Delta_{p\gamma} = -T\sum_{\gamma' i\varepsilon_n}\int \frac{d\mathbf{p}'}{(2\pi)^2} F^{\gamma\gamma'}_{\mathbf{p}\mathbf{p}'} V(|\mathbf{p}-\mathbf{p}'|) G^{(21)}_{\gamma'\gamma'}(\mathbf{p}',i\varepsilon_n). \tag{3}$$

The factor $F^{\gamma\gamma'}_{\mathbf{p}\mathbf{p}'} \equiv |\langle \mathbf{p}\gamma|\mathbf{p}'\gamma'\rangle|^2 = (1+\gamma\gamma'\mathbf{p}\mathbf{p}'/pp')/2$ arises as a result of summation over spinor components of the effective electron wave function in graphene.[29] We use here the static approximation, in which the gap $\Delta_{p\gamma}$ and the statically screened interaction $V(q)$ are real and independent of frequency. Substituting Eqs. (1) and (2) into (3) and performing summation over $\varepsilon_n = \pi T(2n+1)$ and integration over an angle of $\mathbf{p}'$, we get at $T \to 0$

$$\Delta_{p\gamma} = \sum_{\gamma'}\int_0^\infty \frac{p\,dp}{2\pi} U^{(0)}_{\gamma\gamma'}(p,p')\frac{\Delta_{p'\gamma'}}{2E_{p'\gamma'}}, \tag{4}$$

where $U^{(0)}_{\gamma\gamma'}(p,p') = [V_0(p,p') + \gamma\gamma' V_1(p,p')]/2$ is a half-sum of the half-difference of s- and p-wave harmonics of the potential:

$$V_l(p,p') = \int_0^{2\pi}\frac{d\varphi}{2\pi}\cos(l\varphi)V(\sqrt{p^2+p'^2-2pp'\cos\varphi}). \tag{5}$$

At strong coupling, the first harmonic V_1 can be neglected.[29] In this case, the gap functions in conduction and valence bands are equal. We will look for an approximate solution of (4) in a manner similar to that used in Ref. 30: we assume that $\Delta_{p\gamma} = \Delta \times f(p)$, where $f(p)$ is some trial function, satisfying the conditions $f(p_F) = 1$, $f(p) \propto 1/p$ at $p \to \infty$. Fixing in Eq. (4) $p = p_F$ and neglecting V_1, we get the following algebraic equation for the gap Δ at $T = 0$:

$$1 = \int_0^\infty \frac{p'\,dp'}{8\pi} V_0(p_F,p') f(p')\left\{\frac{1}{E_{p'+}} + \frac{1}{E_{p'-}}\right\}. \tag{6}$$

III. SELF-CONSISTENT SUPPRESSION OF THE SCREENING

The statically screened potential of the electron-hole interaction in Eq. (5) in a random phase approximation (the latter if well-applicable in a graphene bilayer due to a large degree of electron state degeneracy[27,32,52]) is[1,24,33]

$$V(q) = \frac{v_q e^{-qD}}{1 - 2v_q\Pi_0(q) + v_q^2\Pi_0^2(q)(1 - e^{-2qD})}. \qquad (7)$$

Here $v_q = 2\pi e^2/\varepsilon q$ is the bare Coulomb attraction, screened by a surrounding medium with dielectric permittivity ε, $\Pi_0(q)$ is a static polarizability of a single graphene layer, and D is the interlayer distance.

The most favorable conditions for the pairing are achieved at small interlayer separation, when $p_F D \ll 1$. In this case, the behavior of the system is determined only by the dimensionless parameter $r_s = e^2/\varepsilon v_F \approx 2.19/\varepsilon$, which specifies the coupling strength, while (7) reduces to

$$V(q) = \frac{v_q}{1 - 2v_q\Pi_0(q)}. \qquad (8)$$

The static polarization operator of doped graphene, calculated without taking into account electron-hole pairing, is[53,54] $\Pi_0(q) = g\mathcal{N}\{-1 + \Theta(q - 2p_F)(q/4p_F)G_<(2p_F/q)\}$. Here $g = 4$ is the degeneracy factor, $\mathcal{N} = \mu/2\pi v_F^2$ is the density of states (per spin projection and valley) at the Fermi level, and $G_<(x) = x\sqrt{1-x^2} - \arccos x$. The long-wavelength asymptotics $\Pi_0(q) \approx -g\mathcal{N}$ provides metallic-like screening at long distances.

Note that at $p_F D \ll 1$, the interaction ceases to depend on a dielectric permittivity of an insulating spacer between graphene layers, since the mean in-plane distance between electrons and holes is much larger than D and thus electric field lines responsible for their interaction pass mainly through the external media around the bilayer. In this case, ε should be taken as a half-sum of dielectric permittivities of the media astride the bilayer (see, e.g., Ref. 55). In suspended two-layer graphene structures, ε can be brought down rather close to unity.

The formation of a condensate of interlayer electron-hole pairs gives rise to a direct response of charge density in one layer on the electric field in the other layer, described by anomalous polarizability Π_a. Normal intralayer polarizabilities Π_n of each graphene layer also change with respect to intrinsic polarizabilities Π_0 due to the appearance of the gap in the energy spectrum. The expression for $V(q)$ at $p_F D \ll 1$ takes the same form as (8), but with the replacement $\Pi_0(q) \to \Pi(q) \equiv \Pi_n(q) + \Pi_a(q)$.

In the random phase approximation, the normal Π_n and anomalous Π_a polarizabilities are calculated as loops consisting of two normal or anomalous Green functions, respectively:

$$\Pi_n(q, i\omega_n) = gT\sum_{\gamma\gamma'\varepsilon_k}\int \frac{d\mathbf{p}}{(2\pi)^2} F_{\mathbf{pp}'}^{\gamma\gamma'} G_{\gamma\gamma}^{(11)}(\mathbf{p}, i\varepsilon_k) G_{\gamma'\gamma'}^{(11)}(\mathbf{p}', i\varepsilon_k + i\omega_n), \qquad (9)$$

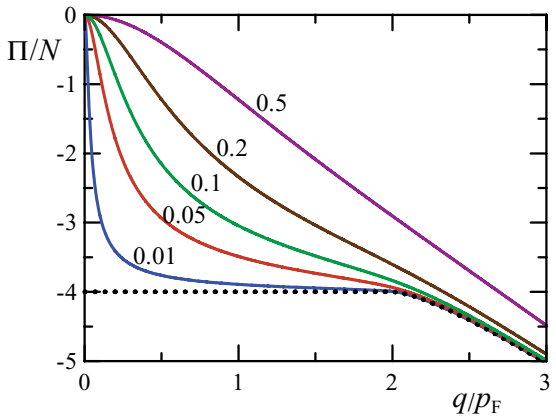

FIG. 1. (Color online) The effective static polarizability Π (in units of the density of states $\mathcal{N}$) in a graphene bilayer with the pairing gap as a function of momentum q at different values of Δ/μ, indicated above corresponding curves (solid lines). Dotted line: the intrinsic static polarizability Π_0 at $\Delta = 0$.

$$\Pi_a(q, i\omega_n) = gT\sum_{\gamma\gamma'\varepsilon_k}\int \frac{d\mathbf{p}}{(2\pi)^2} F_{\mathbf{pp}'}^{\gamma\gamma'} G_{\gamma\gamma}^{(12)}(\mathbf{p}, i\varepsilon_k) G_{\gamma'\gamma'}^{(21)}(\mathbf{p}', i\varepsilon_k + i\omega_n), \qquad (10)$$

where $\mathbf{p}' = \mathbf{p} + \mathbf{q}$. Substituting Eq. (1) into (9) and (10), performing frequency summations, and taking a limit $T \to 0$, we obtain the following expressions for the static polarizabilities $\Pi_{n,a}(q) \equiv \Pi_{n,a}(q, i\omega_n \to 0)$:

$$\Pi_n(q) = -g\sum_{\gamma\gamma'}\int \frac{d\mathbf{p}}{(2\pi)^2} F_{\mathbf{pp}'}^{\gamma\gamma'} \frac{u_{p\gamma}^2 v_{p'\gamma'}^2 + v_{p\gamma}^2 u_{p'\gamma'}^2}{E_{p\gamma} + E_{p'\gamma'}}, \qquad (11)$$

$$\Pi_a(q) = g\sum_{\gamma\gamma'}\int \frac{d\mathbf{p}}{(2\pi)^2} F_{\mathbf{pp}'}^{\gamma\gamma'} \frac{2u_{p\gamma} v_{p\gamma} u_{p'\gamma'} v_{p'\gamma'}}{E_{p\gamma} + E_{p'\gamma'}}. \qquad (12)$$

The sum $\Pi = \Pi_n + \Pi_a$, playing the role of effective polarizability, is plotted in Fig. 1 as calculated numerically according to (11) and (12) at different values of Δ. It is seen that polarizability of the system with the pairing is suppressed at small momenta due to the appearance of the gap. The magnitude and the momentum region of this suppression grow at increasing Δ. The long-wavelength asymptotics $\Pi(q) \approx -g\mathcal{N}q^2/12p_F^2\Delta^2$ indicates that the screening at long distances is absent when $\Delta \neq 0$ and, moreover, the transition from $\Pi(q)$ to $\Pi_0(q)$ at $\Delta \to 0$ is not uniformly continuous.

The absence of a long-range screening causes divergence of the Fermi-surface value $V_0(p_F, p_F)$ of the pairing potential. For this reason, the usual BCS-like recipe, involving the replacement $V_0(p, p') \to V_0(p_F, p_F)$ in the gap equation (4), becomes inapplicable. However, our approach (6) for approximately solving the gap equation is applicable even in this case because the singularity of $V_0(p_F, p')$ at $p' = p_F$ is logarithmic and thus integrable.

In numerical calculations, we use the trial function $f(p) = 1/(|p/p_F - 1| + 1)$ for the gap falling down at characteristic momenta of the order of p_F. For the effective polarizability we use the following approximation:

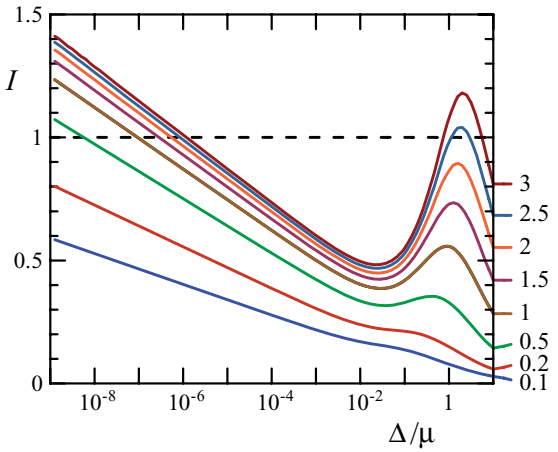

FIG. 2. (Color online) Solid lines: the right-hand side I of the gap equation (6) $I(\Delta) = 1$ as a function of Δ (in logarithmic scale) at different values of r_s, indicated on the right.

$\Pi(q) \approx -g\mathcal{N}q^2/[(12\Delta^2/v_F^2)^{2/3} + q^{4/3}]^{3/2}$, which is close to the numerically calculated $\Pi(q)$ at any Δ and retains its major features—the correct asymptotic at smallest q and the tendency to $-g\mathcal{N}$ at larger q.

The right-hand side I of Eq. (6) is plotted as a function of Δ at various r_s in Fig. 2. The points of intersection $I(\Delta) = 1$ give solutions Δ of the gap equation. In the mean-field approximation, the dependence $I(\Delta)$ should be monotonously decreasing [in the BCS model, $I = \lambda \ln(2w/\Delta)$, where λ and w are the coupling constant and the energy half-width of the pairing region]. Correlation effects make $I(\Delta)$ nonmonotonous at $r_s \gtrsim 0.2$. This can result in the appearance of three solutions of the gap equation, of which only the one with the largest Δ, corresponding to the lowest ground-state energy, will be established in the system.

The maximal gap Δ is plotted in Fig. 3 as a function of r_s. At small enough r_s, the gap value is approximately twice as large as the value obtained without taking into account correlation effects. When r_s exceeds some critical value (about 2.35 in

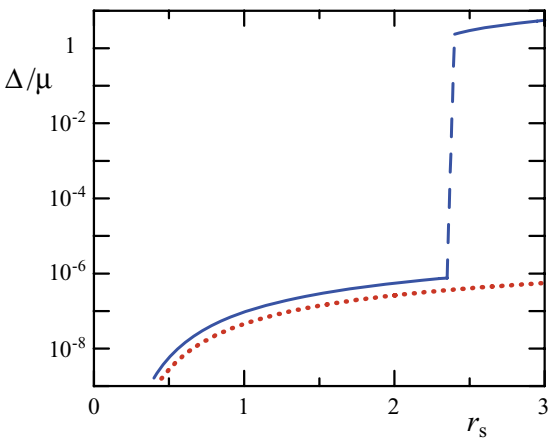

FIG. 3. (Color online) Solid line: the largest value of the gap Δ (in logarithmic scale), found from Eq. (6) at different values of r_s. At $r_s \approx 2.35$, the gap jumps (dashed line) to a much larger value due to the appearance of three solutions of Eq. (6). Dotted line: the gap, calculated in the mean-field approximation.

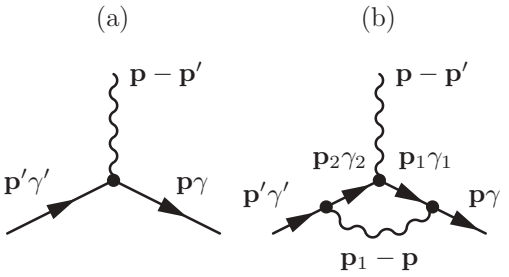

FIG. 4. (a) The bare vertex of the electron-electron Coulomb interaction and (b) the simplest correction to it.

our case), three solutions of (6) appear, and the maximal gap becomes very large and comparable to the chemical potential. The critical value of r_s depends on the details of the model used [in particular, on the form of the trial function $f(p)$]. In our case, it is rather close to the maximal $r_s \approx 2.19$ achievable experimentally at $\varepsilon = 1$ when the graphene bilayer is suspended in vacuum. However, correlation effects can play an important role in the vicinity of the transition to the strongly correlated state even for r_s smaller than the critical value.

IV. VERTEX CORRECTIONS

The bare vertex of the electron-electron Coulomb interaction in graphene [Fig. 4(a)], entering the Gor'kov equations, is $\Gamma^{(0)}_{\gamma'\gamma}(\mathbf{p}',\mathbf{p}) = \langle \mathbf{p}'\gamma'|\mathbf{p}\gamma\rangle$, where the angular factor specific to graphene chiral electrons is[29]

$$\langle \mathbf{p}'\gamma'|\mathbf{p}\gamma\rangle = \begin{cases} \cos\frac{\varphi'-\varphi}{2}, & \gamma = \gamma', \\ i\sin\frac{\varphi'-\varphi}{2}, & \gamma = -\gamma', \end{cases}$$

where φ and φ' are the azimuthal angles of $\mathbf{p}$ and $\mathbf{p}'$.

The simplest correction $\Gamma^{(1)}$ to $\Gamma^{(0)}$ is shown diagrammatically in Fig. 4(b). We take the bare Green functions $G^{(0)}_{\gamma_2\gamma_2}(\mathbf{p}_2, i\varepsilon_2)$ and $G^{(0)}_{\gamma_1\gamma_1}(\mathbf{p}_1, i\varepsilon_1)$ as internal electron lines of this vertex, and the Coulomb interaction as the internal wavy line. Moreover, we consider only the static vertex, i.e., the vertex function at zero frequencies: $\Gamma^{(1)}_{\gamma'\gamma}(\mathbf{p}',\mathbf{p}) \equiv \Gamma^{(1)}_{\gamma'\gamma}(\mathbf{p}', i\varepsilon' \to 0, \mathbf{p}, i\varepsilon \to 0)$. After frequency summation in the internal loop, we get in a zero-temperature limit $T \to 0$,

$$\Gamma^{(1)}_{\gamma'\gamma}(\mathbf{p}',\mathbf{p}) = \sum_{\gamma_1\gamma_2} \int \frac{d\mathbf{p}_1}{(2\pi^2)} \langle \mathbf{p}'\gamma'|\mathbf{p}_2\gamma_2\rangle\langle \mathbf{p}_2\gamma_2|\mathbf{p}_1\gamma_1\rangle \times \langle \mathbf{p}_1\gamma_1|\mathbf{p}\gamma\rangle V(|\mathbf{p}_1 - \mathbf{p}|) \frac{\Theta(\xi_{p_1\gamma_1}) - \Theta(\xi_{p_2\gamma_2})}{\xi_{p_1\gamma_1} - \xi_{p_2\gamma_2}}, \quad (13)$$

where $\mathbf{p}_2 = \mathbf{p}_1 + \mathbf{p}' - \mathbf{p}$ and $\Theta(x)$ is a unit step function.

We can use the bare Coulomb interaction $2\pi e^2/\varepsilon q$ as $V(q)$ in Eq. (13), but in this case the integral over $\mathbf{p}_1$ diverges at small momenta. To avoid the divergence, we take the statically screened interaction (8) as $V(q)$.

Substitution of the vertex correction (13) into Gor'kov equations results in the correction to the potential,

$$U^{(1)}_{\gamma\gamma'}(p,p') = \int_0^{2\pi} \frac{d\varphi'}{2\pi} \langle \mathbf{p}\gamma|\mathbf{p}'\gamma'\rangle \Gamma^{(1)}_{\gamma'\gamma}(\mathbf{p}',\mathbf{p}), \quad (14)$$

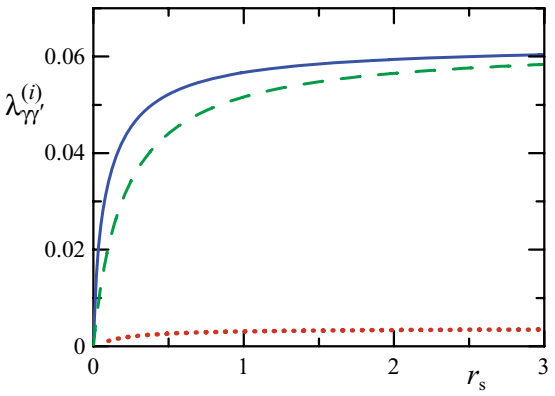

FIG. 5. (Color online) The dimensionless second-order correction $\lambda^{(1)}_{++}$ (dotted line) to the coupling constant as a function of r_s in comparison with the first-order intraband $\lambda^{(0)}_{\gamma\gamma}$ (solid line) and interband $\lambda^{(0)}_{\gamma,-\gamma}$ (dashed line) coupling constants.

added to $U^{(0)}_{\gamma\gamma'}(p,p')$ in the gap equation (4). To estimate the effect of vertex corrections on the pairing, we compare the second-order correction to the coupling constant on the Fermi surface $\lambda^{(1)}_{++} = \mathcal{N}U^{(1)}_{++}(p_F,p_F)$ with its first-order value $\lambda^{(0)}_{\gamma\gamma'} = \mathcal{N}U^{(0)}_{\gamma\gamma'}(p_F,p_F)$.

In Fig. 5, the conduction-band component of the correction $\lambda^{(1)}_{++}$ is plotted as a function of r_s. Its other components ($\lambda^{(1)}_{--}$ and $\lambda^{(1)}_{\gamma,-\gamma}$) are very close to it and thus are not shown. For comparison, the first-order coupling constants in the intraband ($\lambda^{(0)}_{\gamma\gamma}$) and interband ($\lambda^{(0)}_{\gamma,-\gamma}$) channels are also plotted (these quantities were studied in detail in Ref. 29). It is seen that the second-order vertex corrections amount only to about 5% of the first-order coupling constants and thus can be neglected.

V. CONCLUSIONS

We considered the role of correlation effects in the pairing of spatially separated electrons and holes in a graphene bilayer in the multiband regime at strong coupling. The first effect is the self-consistent suppression of the screening of electron-hole interaction due to the appearance of the gap and the order parameter. Its most remarkable consequence is the absence of screening at long distances at any nonzero gap, which makes the usual BCS method inapplicable due to the divergence of the interaction at the Fermi surface.

Therefore, we performed numerical calculations with full momentum integration to solve the gap equation. We found that at small coupling strengths, correlations increase the gap by a factor of 2. However, at a coupling strength above some threshold, the gap sharply increases by several orders of magnitude, indicating a transition of the system into a strongly correlated state.

A quantitative description of this transition requires extensive calculations, including the momentum and frequency dependence of the gap functions. Moreover, additional factors such as renormalization of the chemical potential[34] should be taken into account when the gap turns out to be very large. In our simple model, the critical value of the coupling strength is only slightly larger than the maximal value achievable in experiments. More complicated treatment can lead to a revision of this critical value. Nevertheless, our results indicate that the possibility of the transition to the strongly correlated state with a large gap in realizable conditions is not excluded. The correlation effects can also manifest themselves in the vicinity of this transition. Such sharp transition can be associated with a Cooper pair condensate analog of exciton liquid formation.[46]

It should be noted that correlation effects of a similar type can, in principle, arise in any system with electron-hole pairing. It can be particularly interesting in the case of thin films of a topological insulator with asymmetric doping of opposite surfaces, where the pairing of Dirac electrons and holes accompanied by the formation of exciton condensate with unusual superfluid and topological properties can occur.[55–57]

We have also considered the role of vertex corrections at strong coupling. The simplest correction to the interaction vertex was calculated numerically in the static approximation and was shown to enhance the pairing slightly by about 5%.

Note added. After this article was submitted, we became aware of Ref. 58, which contains similar results.

ACKNOWLEDGMENTS

This work was supported by the Russian Foundation for Basic Research. One of the authors (A.A.S.) was also supported by the Dynasty Foundation and by a grant from the President of the Russian Federation for Young Scientists, No. MK-5288.2011.2.

*lozovik@isan.troitsk.ru

[1] Yu. E. Lozovik and V. I. Yudson, Pis'ma Zh. Eksp. Teor. Fiz. **22**, 556 (1975) [JETP Lett. **22**, 274 (1975)]; Zh. Eksp. Teor. Fiz. **71**, 738 (1976) [Sov. Phys. JETP **44**, 389 (1976)]; Solid State Commun. **22**, 117 (1977); **19**, 391 (1976).

[2] S. I. Shevchenko, Phys. Rev. Lett. **72**, 3242 (1994).

[3] Yu. E. Lozovik and A. V. Poushnov, Phys. Lett. A **228**, 399 (1997).

[4] Yu. E. Lozovik and I. V. Ovchinnikov, Phys. Rev. B **66**, 075124 (2002).

[5] A. V. Balatsky, Y. N. Joglekar, and P. B. Littlewood, Phys. Rev. Lett. **93**, 266801 (2004).

[6] L. V. Keldysh and Yu.V. Kopaev, Fiz. Tverd. Tela (Leningrad) **6**, 2791 (1965) [Sov. Phys. Solid State **6**, 2219 (1965)].

[7] J. P. Eisenstein and A. H. MacDonald, Nature (London) **432**, 691 (2004).

[8] D. W. Snoke, Phys. Status Solidi B **238**, 389 (2003).

[9] V. B. Timofeev, Usp. Fiz. Nauk **175**, 315 (2005) [Phys. Usp. **48**, 295 (2005)].

[10] L. V. Butov, J. Phys.: Condens. Matter **16**, R1577 (2004).

[11] P. B. Littlewood, P. R. Eastham, J. M. J. Keeling, F. M. Marchetti, and M. H. Szymanska, J. Phys.: Condens. Matter **16**, S3597 (2004).

[12] J. A. Seamons, C. P. Morath, J. L. Reno, and M. P. Lilly, Phys. Rev. Lett. **102**, 026804 (2009).

[13]K. S. Novoselov, A. K. Geim, S. V. Morozov, D. Jiang, M. I. Katsnelson, I. V. Grigorieva, S. V. Dubonos, and A. A. Firsov, Nature (London) **438**, 197 (2005).
[14]A. H. Castro Neto, F. Guinea, N. M. R. Peres, K. S. Novoselov, and A. K. Geim, Rev. Mod. Phys. **81**, 109 (2009).
[15]H. Schmidt, T. Lüdtke, P. Barthold, E. McCann, V. I. Falko, and R. J. Haug, Appl. Phys. Lett. **93**, 172108 (2008).
[16]H. Schmidt, T. Lüdtke, P. Barthold, and R. J. Haug, Phys. Rev. B **81**, 121403(R) (2010).
[17]S. Kim, I. Jo, J. Nah, Z. Yao, S. K. Banerjee, and E. Tutuc, Phys. Rev. B **83**, 161401 (2011).
[18]C. R. Dean, A. F. Young, I. Meric, C. Lee, L. Wang, S. Sorgenfrei, K. Watanabe, T. Taniguchi, P. Kim, K. L. Shepard, and J. Hone, Nat. Nano. **5**, 722 (2010).
[19]C. R. Dean, A. F. Young, P. Cadden-Zimansky, L. Wang, H. Ren, K. Watanabe, T. Taniguchi, P. Kim, J. Hone, and K. L. Shepard, Nat. Phys. **7**, 693 (2011).
[20]J. Xue, J. Sanchez-Yamagishi, D. Bulmash, P. Jacquod, A. Deshpande, K. Watanabe, T. Taniguchi, P. Jarillo-Herrero, and B. J. LeRoy, Nat. Mater. **10**, 282 (2011).
[21]A. S. Mayorov, R. V. Gorbachev, S. V. Morozov, L. Britnell, R. Jalil, L. A. Ponomarenko, P. Blake, K. S. Novoselov, K. Watanabe, T. Taniguchi, and A. K. Geim, Nano Lett. **11**, 2396 (2011).
[22]D. A. Abanin, S. V. Morozov, L. A. Ponomarenko, R. V. Gorbachev, A. S. Mayorov, M. I. Katsnelson, K. Watanabe, T. Taniguchi, K. S. Novoselov, L. S. Levitov, and A. K. Geim, Science **332**, 328 (2011).
[23]M. I. Katsnelson, Phys. Rev. B **84**, 041407 (2011).
[24]Yu. E. Lozovik and A. A. Sokolik, Pis'ma Zh. Eksp. Teor. Fiz. **87**, 61 (2008) [JETP Lett. **87**, 55 (2008)].
[25]H. Min, R. Bistritzer, J.-J. Su, and A. H. MacDonald, Phys. Rev. B **78**, 121401(R) (2008).
[26]C.-H. Zhang and Y. N. Joglekar, Phys. Rev. B **77**, 233405 (2008).
[27]M. Yu. Kharitonov and K. B. Efetov, Phys. Rev. B **78**, 241401(R) (2008).
[28]Yu. E. Lozovik and A. A. Sokolik, Phys. Lett. A **374**, 326 (2009).
[29]Yu. E. Lozovik and A. A. Sokolik, Eur. Phys. J. B **73**, 195 (2009).
[30]Yu. E. Lozovik, S. L. Ogarkov, and A. A. Sokolik, Philos. Trans. R. Soc. London, Ser. A **368**, 5417 (2010).
[31]R. Bistritzer, H. Min, J.-J. Su, and A. H. MacDonald, arXiv:0810.0331 [cond-mat].
[32]M. Yu. Kharitonov and K. B. Efetov, Semicond. Sci. Technol. **25**, 034004 (2010).
[33]M. P. Mink, H. T. C. Stoof, R. A. Duine, and A. H. MacDonald, Phys. Rev. B **84**, 155409 (2011).
[34]P. Nozières and S. Schmitt-Rink, J. Low Temp. Phys. **59**, 195 (1985).
[35]Yu. E. Lozovik and A. A. Sokolik, J. Phys.: Conf. Ser. **129**, 012003 (2008).
[36]O. L. Berman, Yu. E. Lozovik, and G. Gumbs, Phys. Rev. B **77**, 155433 (2008).
[37]O. L. Berman, R. Ya. Kezerashvili, and K. Ziegler, Phys. Rev. B **85**, 035418 (2012).
[38]P. W. Anderson, Phys. Rev. **112**, 1900 (1958).
[39]R. E. Prange, Phys. Rev. **129**, 2495 (1962).
[40]F. Marsiglio, Phys. Rev. B **47**, 5419 (1993).
[41]H.-Y. Kee and C. M. Varma, Phys. Rev. Lett. **79**, 4250 (1997).
[42]A. N. Kozlov and L. A. Maksimov, Zh. Eksp. Teor. Fiz. **48**, 1184 (1965) [Sov. Phys. JETP **21**, 790 (1965)].
[43]R. Zimmermann, Phys. Status Solidi B **76**, 191 (1976).
[44]A. P. Silin, Fiz. Tverd. Tela (Leningrad) **19**, 134 (1977) [Sov. Phys. Solid State **19**, 77 (1977)].
[45]P. Nozières and C. Comte, J. Phys. **43**, 1083 (1982).
[46]Yu. E. Lozovik and O. L. Berman, Zh. Eksp. Teor. Fiz. **111**, 1879 (1997) [JETP **84**, 1027 (1997)].
[47]C. Grimaldi, L. Pietronero, and S. Strassler, Phys. Rev. Lett. **75**, 1158 (1995).
[48]J. Gonzalez, F. Guinea, and M. A. H. Vozmediano, Nucl. Phys. B **424**, 595 (1994).
[49]V. N. Kotov, B. Uchoa, and A. H. Castro Neto, Phys. Rev. B **78**, 035119 (2008).
[50]J. Sabio, J. Nilsson, and A. H. Castro Neto, Phys. Rev. B **78**, 075410 (2008).
[51]V. Juričić, O. Vafek, and I. F. Herbut, Phys. Rev. B **82**, 235402 (2010).
[52]S. M. Apenko, D. A. Kirzhnits, and Yu. E. Lozovik, Phys. Lett. A **92**, 107 (1982).
[53]B. Wunsch, T. Stauber, F. Sols, and F. Guinea, New J. Phys. **8**, 318 (2006).
[54]E. H. Hwang and S. Das Sarma, Phys. Rev. B **75**, 205418 (2007).
[55]D. Tilahun, B. Lee, E. M. Hankiewicz, and A. H. MacDonald, Phys. Rev. Lett. **107**, 246401 (2011).
[56]B. Seradjeh, J. E. Moore, and M. Franz, Phys. Rev. Lett. **103**, 066402 (2009).
[57]D. K. Efimkin, Yu. E. Lozovik, and A. A. Sokolik, arXiv:1207.1817v2 [cond-mat.mes-hall].
[58]I. Sodemann, D. A. Pesin, and A. H. MacDonald, Phys. Rev. B **85**, 195136 (2012).